Anti-Windup PID Controller With Integral State Predictor for Variable-Speed Motor Drives

Hwi-Beom Shin, *Member, IEEE*, and Jong-Gyu Park

***Abstract*—The windup phenomenon appears and results in performance degradation when the proportional-integral-derivative (PID) controller output is saturated. Integral windup is analyzed on the PI plane, and a new anti-windup PID controller is proposed to improve control performance of variable-speed motor drives and is experimentally applied to the speed control of a vector–controlled induction motor driven by a pulse width-modulated voltage source inverter. The steady-state value of the integral state is predicted while the PID controller output is saturated, and this value is utilized as an initial value of the integral state when the PID controller begins to operate in a linear range. Simulation and experiments result in more similar speed responses against load conditions and step reference change over conventional anti-windup schemes. Control performance, such as overshoot and settling time, is very similar to that determined by PID gain in the linear range.**

***Index Terms*—Anti-windup proportional-integral-derivative (PID) control, integral state prediction, variable-speed motor drives.**

I. Introduction

THE proportional-integral-derivative (PID) control scheme has been widely used as a cascade form in variable-speed motor drives. Current control is employed in an inner feedback loop for the purpose of fast dynamics and peak current protection, while the outer speed controller generates a current command for the current controller. This current command is limited to a prescribed maximum value due to converter protection, magnetic saturation, and overheating of the motor. Therefore, saturation nonlinearity exists in the speed control loop. Since the PID controller is usually designed in a linear region that ignores control input limitation, closed-loop performance will significantly deteriorate in terms of expected linear performance. This performance deterioration is referred to as windup phenomenon, which causes large overshoot, slow settling time, and sometimes even instability in speed response [1]–[4].

To overcome this windup phenomenon, a number of anti-windup techniques have been proposed in related literature and may be classified into three categories: conditional integration, tracking back calculation, and limited integrator schemes. In conditional integration schemes [5]–[7], the integral action is suspended when control input is saturated and only the PD control is activated. When the control input lies within the saturation limit, the PID control is effective, and a zero steady-state error can be guaranteed. The initial value of the integrator in PI control is properly calculated by using the previous steady-state value of the integrator in [5]. The difference between saturated and unsaturated control input signals is used to generate a feedback signal to act on integrator input for the tracking back calculation methods [1], [8]–[11]. Transient performance such as overshoot depends heavily upon feedback gain of the control difference rather than PID gains. Both conditional integration and tracking back calculation are combined in [12]–[14]. For the limited integrator scheme [15], the integrator value is limited by feeding the control back with a high-gain dead zone to guarantee operation in the linear range. For saturation limits, this scheme is the same as the back calculation method.

In this paper, integral windup is analyzed on the PI plane and a newly proposed anti-windup PID controller is suggested for variable-speed motor drives. The steady-state value of the integral state is predicted while PID controller output is saturated, and this value is utilized as an initial value of the integral state when the PID controller begins to operate in the linear range. With the proposed anti-windup technique, integral windup is minimized and speed response is determined by the selected PID gain only. Hence, similar responses are obtained without regard to load conditions or step reference change, resulting in expectations that control performance will easily improve.

II. Anti-Windup PID Control

Current controllers are commonly designed to have much faster dynamics than speed controllers. If a fast current control scheme is employed, the current dynamics is negligible and the variable-speed motor drive can be represented as a first-order system given by [13]

$$\frac{d\omega_r}{dt} = -\frac{1}{\tau_m}\omega_r + k_t v - T_l \tag{1}$$

where $\tau_m = J/B$, $k_t = k_T/J$, $T_l = T_L/J$, and v denotes the plant input, namely, the torque-producing current. It is assumed that the plant input v is limited by saturation nonlinearity as

$$v = \begin{cases} U_h & \text{if } u > U_h \\ u & \text{if } U_l \le u \le U_h \\ U_l & \text{if } u < U_l \end{cases} \tag{2}$$

where u represents the controller output. In the following, it will be called the linear range and the saturation range when $u = v$ and $u \neq v$, respectively.

Manuscript received October 26, 2010; revised February 28, 2011 and June 7, 2011; accepted July 17, 2011. Date of publication August 8, 2011; date of current version October 25, 2011. This work was supported by KESRI(11103), which is funded by Korea Western Power Co.

H.-B. Shin is with the Department of Electrical Engineering, Gyeongsang National University, Jinju 660-701, Korea (e-mail: hbshin@gnu.ac.kr).

J.-G. Park is with the Department of Electricity, Gyeongnam Provincial Namhae College, Gyeongnam 668-801, Korea.

Digital Object Identifier 10.1109/TIE.2011.2163911

A. PID Control Responses According to Initial Values of Integral State

It is assumed that the PID controller operates in the linear range. The PID control is then expressed as

$$u = k_p e + k_i q + k_d \dot{e} \tag{3}$$

where k_p, k_i, and k_d denote proportional, integral, and derivative gains, respectively. The error is

$$e = \omega_r^* - \omega_r \tag{4}$$

where ω_r^* denotes the speed command. The integral state q is given as

$$\dot{q} = e. \tag{5}$$

For the step change of the speed command, the error dynamics can be written, by substituting (4) and (5) into (1), as

$$\dot{e} = -\frac{1}{\tau_m} e - k_t u + T_l + \frac{1}{\tau_m} \omega_r^*. \tag{6}$$

If the PID-controlled system is stable, the integral state in the steady state can be expressed, from (3), (5), and (6), as

$$q_{ss} = \left(T_l + \frac{1}{\tau_m} \omega_r^* \right) / k_t k_i \tag{7}$$

where the subscript ss denotes the steady-state value. It is noted that the steady-state value of the integral state includes external load torque and the speed command. Substituting (3) and (7) into (6) yields the error dynamics as

$$(1 + k_t k_d)\dot{e} = -\left(\frac{1}{\tau_m} + k_t k_p \right) e + k_t k_i (q_{ss} - q). \tag{8}$$

Taking Laplace transformation on (5) and (8) yields the error transfer function given as

$$E(s) = \frac{s}{s^2 + \left(\frac{1/\tau_m + k_t k_p}{1 + k_t k_d} \right) s + \frac{k_t k_i}{1 + k_t k_d}} e(0) + \frac{k_t k_i / (1 + k_t k_d)}{s^2 + \left(\frac{1/\tau_m + k_t k_p}{1 + k_t k_d} \right) s + \frac{k_t k_i}{1 + k_t k_d}} \{ q_{ss} - q(0) \}. \tag{9}$$

Error response depends on PID gain, initial error value, and the difference between initial and steady-state values of the integral state. Basically, PID-controlled system stability depends on PID gains. Fig. 1 shows the output responses of PID control according to different steady-state values of the integral state where the initial integral states have the same value and controller output is not saturated. It can be seen that transient responses such as overshoot and settling time are influenced by the steady-state value of the integral state: namely, external load torque and the speed command.

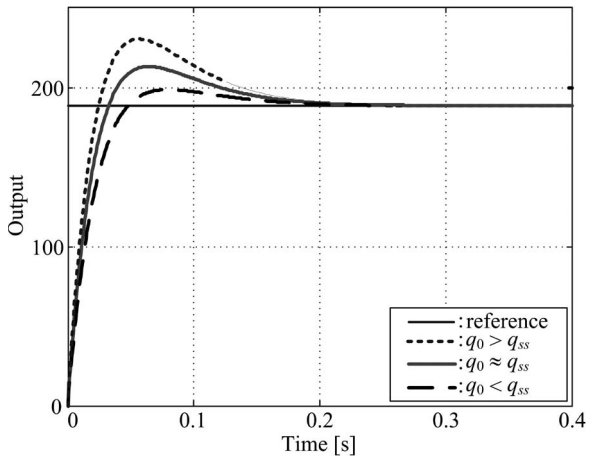

Fig. 1. PID responses without input saturation according to differences between initial and steady-state values of the integral state.

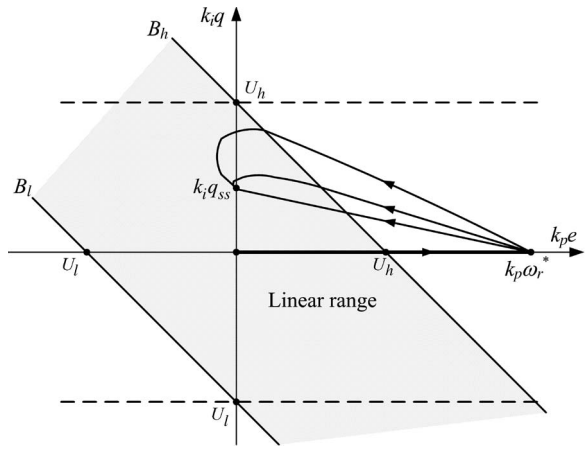

Fig. 2. Linear range and error trajectories for step command on the PI plane under identical PID gain.

B. Anti-Windup PID Responses on the PI Plane

If the plant input constraint in (2) is considered, the upper and lower boundaries of the linear range can be found from (3) as

$$B_h: \quad k_i q \approx -k_p e + U_h \tag{10}$$

$$B_l: \quad k_i q \approx -k_p e + U_l. \tag{11}$$

In the above equations, derivative control is ignored because its contribution is usually much smaller than the proportional and integral controls. Fig. 2 shows several error trajectories on the PI plane whose coordinate consists of the proportional and integral actions: namely, $k_p e$-$k_i q$. The shaded area denotes the linear range. When the PID control system is stable, the steady-state value of the integral state $k_i q_{ss}$ satisfies the following condition:

$$U_l \leq k_i q_{ss} \leq U_h. \tag{12}$$

For the step command, the error trajectories of the PID control move into the saturation range rapidly and the error begins to converge to zero via a saturated control input. This interval affects only the rise time in control performance specifications.

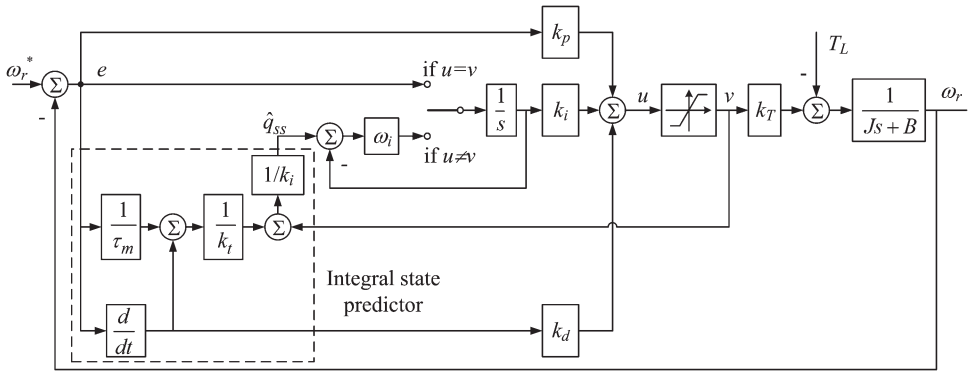

Fig. 3. Proposed anti-windup PID control with integral state prediction.

The error trajectory touches the linear range boundary if the attractive condition is satisfied [13]. The error dynamics are dependent upon both the selected PID gain and the touch conditions like error or the integral state. Of these, integral state value dominates transient overshoot.

It can be seen from (9) and Fig. 2 that overshoot is connected to the relative position of the integral state against the steady-state point. When the integral state on the linear range boundary is higher than the steady-state value, large overshoot is apt to occur in the error response. On the other hand, error response may slow down as the integral state on the linear range boundary is lower than the steady-state value. It is noted that improper touch conditions can deteriorate error response even though the proper PID gain is selected. Touch conditions vary according to anti-windup scheme.

C. Proposed Anti-Windup PID Control With Integral State Prediction

PID gains satisfying the desired control specifications are usually determined by considering worst case scenarios like no-load or full-load conditions [1]. When PID gains are chosen to meet no load specifications, output response may be quite overdamped at full load and settling time may be prolonged. When PID gains are chosen to meet full-load specifications, there may be a larger overshoot and longer settling time at no load in output response. It is desirable that the integral state is initially loaded with its steady-state value at the beginning of the linear range to obtain an output response unaffected by the load conditions. Therefore, the steady-state value of the integral state will be predicted while the PID control operates in the saturation range. The predicted value is used as an initial value of the integral state when the PID controller operates in the linear range.

The proposed PID control is given as

$$u = k_p e + k_i q + k_d \dot{e} \tag{13}$$

where the integral state of PID control is updated as

$$\dot{q} = \begin{cases} e & \text{if } u = v \\ \omega_i(\hat{q}_{ss} - q) & \text{if } u \neq v. \end{cases} \tag{14}$$

In the above equation, ω_i is the positive parameter of the low-pass filter for loading the initial value into the integrator, while $\hat{q}_{ss}$ denotes the predicted steady-state value of the integral state.

TABLE I
PARAMETERS OF INDUCTION MOTOR

1[hp], 220[V], 4[pole], 60[Hz], 1730[rpm]		
R_s = 1.985[Ω],	R_r = 1.73[Ω],	X_m = 57.65[Ω]
X_s = 59.6[Ω],	X_r = 60.57[Ω],	V_{dc} = 310[V]
J = 5.0 x 10^{-3}[Kgm^2],	B = 0.8 x 10^{-3}[Kgm^2/s]	
τ_m = 6.25 [s],	k_T = 1.27 [Nm/A]	

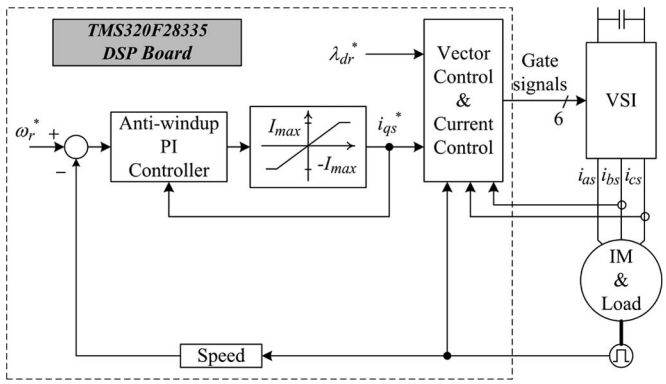

Fig. 4. Block diagram of vector-controlled induction motor drive using anti-windup PID speed controller.

When the PID controller operates in the saturation range, the error dynamics can be expressed as

$$\dot{e} = -\frac{1}{\tau_m} e - k_t v + k_t k_i q_{ss} \quad \text{where} \quad v \in \{U_h, U_l\}. \tag{15}$$

The amount of error is measurable and the system constants τ_m and k_t can be estimated accurately. The integral state within the saturation range can therefore be predicted from (15) as

$$\hat{q}_{ss} = \frac{1}{k_i}\left\{\frac{1}{k_t}\left(\dot{e} + \frac{1}{\tau_m} e\right) + v\right\} \quad \text{where} \quad v \in \{U_h, U_l\}. \tag{16}$$

The integral state loading dynamics can be expressed as

$$\frac{q(s)}{\hat{q}_{ss}(s)} = \frac{1}{s/\omega_i + 1}. \tag{17}$$

The integral state loading time can be determined by adjusting the bandwidth parameter ω_i properly. Usually, low-pass filter

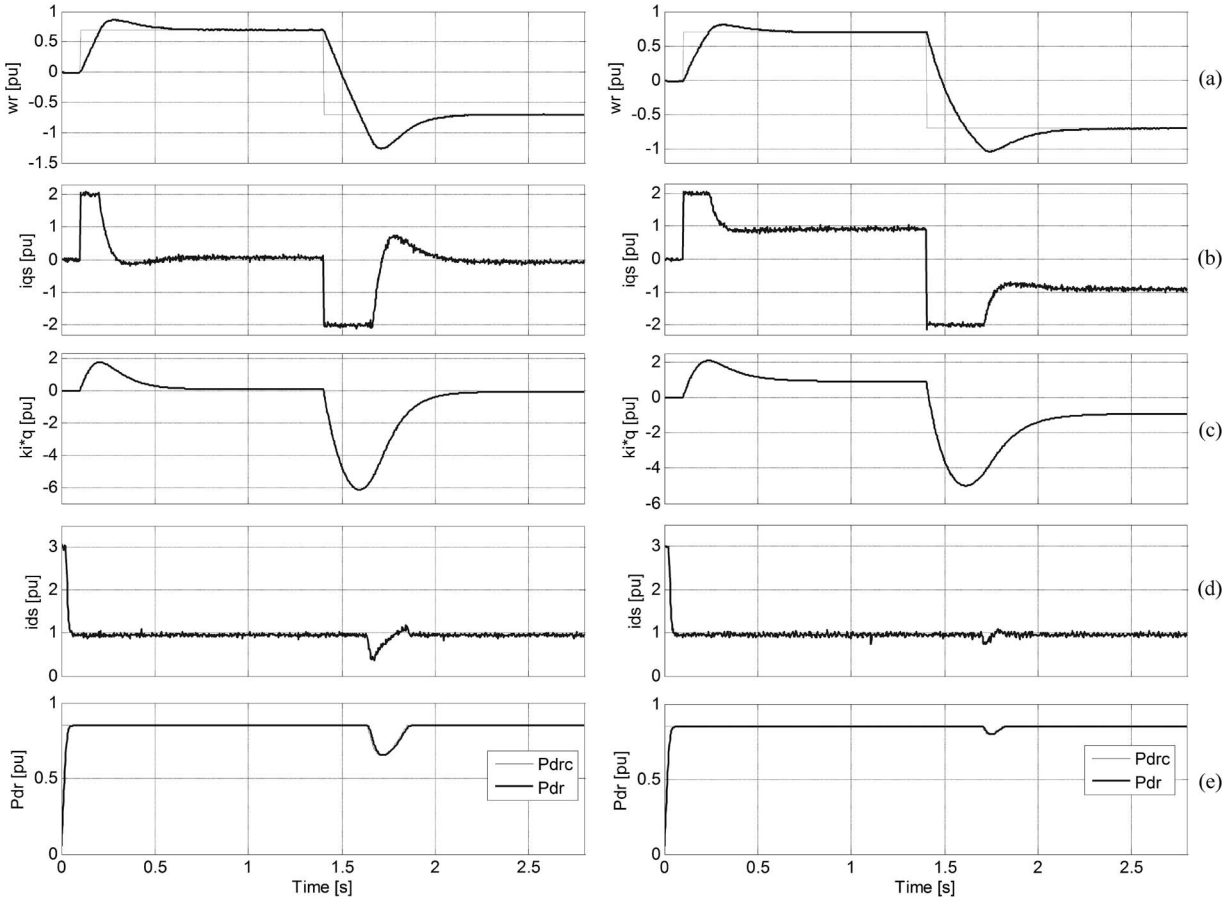

Fig. 5. Experimental results of PID control without anti-windup scheme under no-load (left) and full-load (right) conditions. (a) Speed. (b) Torque producing current. (c) Integral control. (d) d-axis flux producing current, (e) d-axis rotor flux.

bandwidth is much higher than that of the PID-controlled system. Since the integral state prediction in (16) includes an error derivative, low-pass filter bandwidth is constrained by derivative noise.

Fig. 3 shows the proposed anti-windup PID control with integral state prediction. When the PID control operates in the linear range, output error is connected to integrator input. When the PID control operates in the saturation range, the integral state is reset to a predicted steady-state value through a low-pass filter to prevent abrupt integral state changes and reduce prediction noise.

III. Simulation and Experimental Results

The proposed anti-windup PID controller has been applied to the speed control of an induction motor driven by a pulse width-modulated (PWM)-voltage source inverter (VSI) and experimentally verified and compared with the conventional schemes of conditional integration and tracking back calculation. The parameters of a 1 hp induction motor are listed in Table I. In the vector control method [16], the induction motor is controlled like a separately excited dc motor. The d-axis stator current controls the d-axis rotor flux λ_{dr} and the q-axis stator current i_{qs} produces the shaft torque T_e such as

$$T_e = k_T i_{qs} \tag{18}$$

where the torque constant k_T is given as

$$k_T = \frac{X_m}{X_r}\lambda_{dr}. \tag{19}$$

When the d-axis rotor flux is controlled to maintain a constant value and only the mechanical dynamics is considered, the vector-controlled induction motor becomes the first-order system given by (1). When the integral state is predicted by using (16), the error derivative term is included and the derivative noise increases. The integral state of the stable PID control is bounded as (12). To overcome error derivative noise from the reference step change, the predicted integral state is limited as

$$\hat{q}_{ss} = \begin{cases} U_h/k_i & \text{if } k_i\hat{q}_{ss} > U_h \\ U_l/k_i & \text{if } k_i\hat{q}_{ss} < U_l. \end{cases} \tag{20}$$

It is desirable that the bandwidth parameter ω_i is chosen as 3$\sim$5 times the speed loop bandwidth.

Fig. 4 is a block diagram of an experimental system. The control algorithm was fully implemented in software with a TMS320F28335 DSP, which includes A/D converters and a three-phase PWM generator. The three-phase currents are controlled to settle within 2 ms by using a synchronous PI regulator, while the rotor flux is controlled to settle within 30 ms. The space vector PWM method is used with PWM frequency at 10 kHz. The sampling times of the current and the speed control

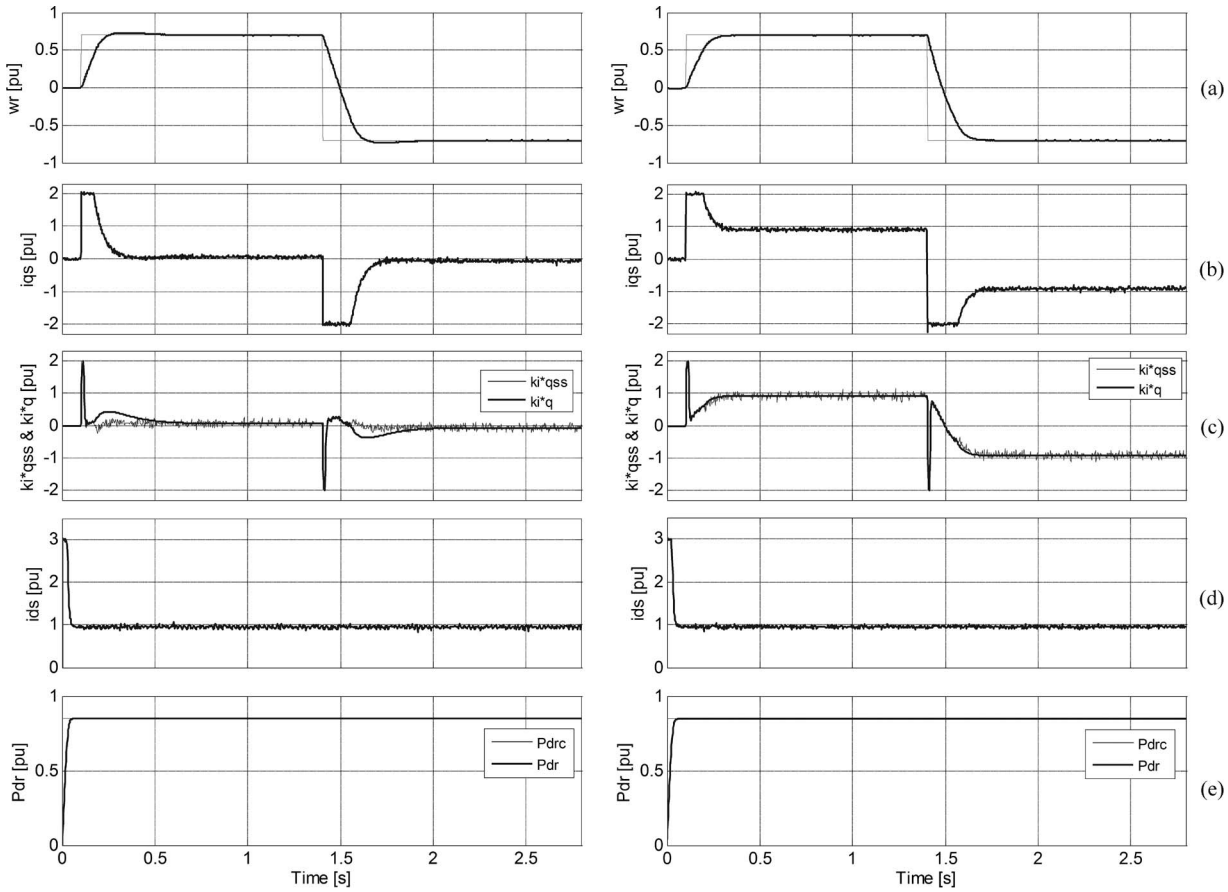

Fig. 6. Experimental results of the proposed anti-windup PID control under no-load (left) and full-load (right) conditions. (a) Speed. (b) Torque producing current. (c) Predicted and actual integral controls. (d) d-axis flux producing current. (e) d-axis rotor flux.

loops are 0.05 ms and 2 ms, respectively. The shaft encoder has 1000 pulses per revolution. The 0.75 kW BLDC generator is mechanically linked to the induction motor for generating the load torque. The resistor is electrically connected to the generator. The load torque is proportional to the motor speed as

$$T_L = T_{L,rated} \cdot (\omega_r/\omega_{r,rated}). \tag{21}$$

Therefore, the load torque is not constant in the experimental setup but its steady-state value is constant. In the following experiments and simulations, the torque-producing current i_{qs} is limited to ± 2 pu, and the flux-producing current i_{ds} is limited to 3 pu. The per-unit values are scaled with 1800 r/min for speed and 2.77 A for current. The d-axis rotor flux is controlled to settle within 30 ms and the magnitude is $\lambda_{dr}^* = 0.85$ pu at $t = 0$ s. The parameter ω_i is chosen as giving the loading time of 15 ms.

Fig. 5 shows the experimental results of the PID control without the anti-windup scheme under no-load and full-load conditions, where the PID gains are selected as $k_p = 7.351$, $k_i = 46.48$, and $k_d = 0.005$. The speed command $\omega_r^* = 0.7$ pu at $t = 0.1$ s and $\omega_r^* = -0.7$ pu at $t = 1.4$ s. Integrating speed error during input saturation causes integral windup and transient performance to deviate significantly from what has been designed. The capacitor bank in the dc link of the PWM inverter may suffer overvoltage due to significant overshoot. If the inverter has no overvoltage protection circuit, the capacitor can be destroyed. When PID gain is selected to obtain faster speed response, the integral windup becomes more serious, and overvoltage protection is actually activated. During speed reversal, the speed response exceeds 1 pu, and the d-axis flux controller operates in the flux weakening region as shown in Fig. 5(e).

Fig. 6 shows experimental results of the proposed anti-windup scheme under no-load and full-load conditions, where the same experimental conditions in Fig. 5 are used. It can be seen in Fig. 6(c) that the integral state predictor predicts well the steady-state value at both no-load and full-load during the saturation range. The integral state is also loaded with the predicted value before the PID control enters into the linear range. Therefore, it is expected that the speed response of the proposed anti-windup scheme is determined only by the PID gain during the linear range. It can be seen in Fig. 6(a) that the speed responses are similar without respect to the load conditions in the linear range.

Fig. 7 compares the simulated and experimental results under no-load conditions with different anti-windup methods, where $\omega_r^* = 0.96$ pu at $t = 0$ s and $\omega_r^* = -0.96$ pu at $t = 0.5$ s. PID gains are selected as $k_p = 12.3$, $k_i = 130$, and $k_d = 0$. Anti-windup gain is selected as $1/k_p$ for tracking back calculation [1] and the combined anti-windup scheme [11]. For simulated comparison of some anti-windup schemes, the first-order mechanical model in (1) is simulated by using

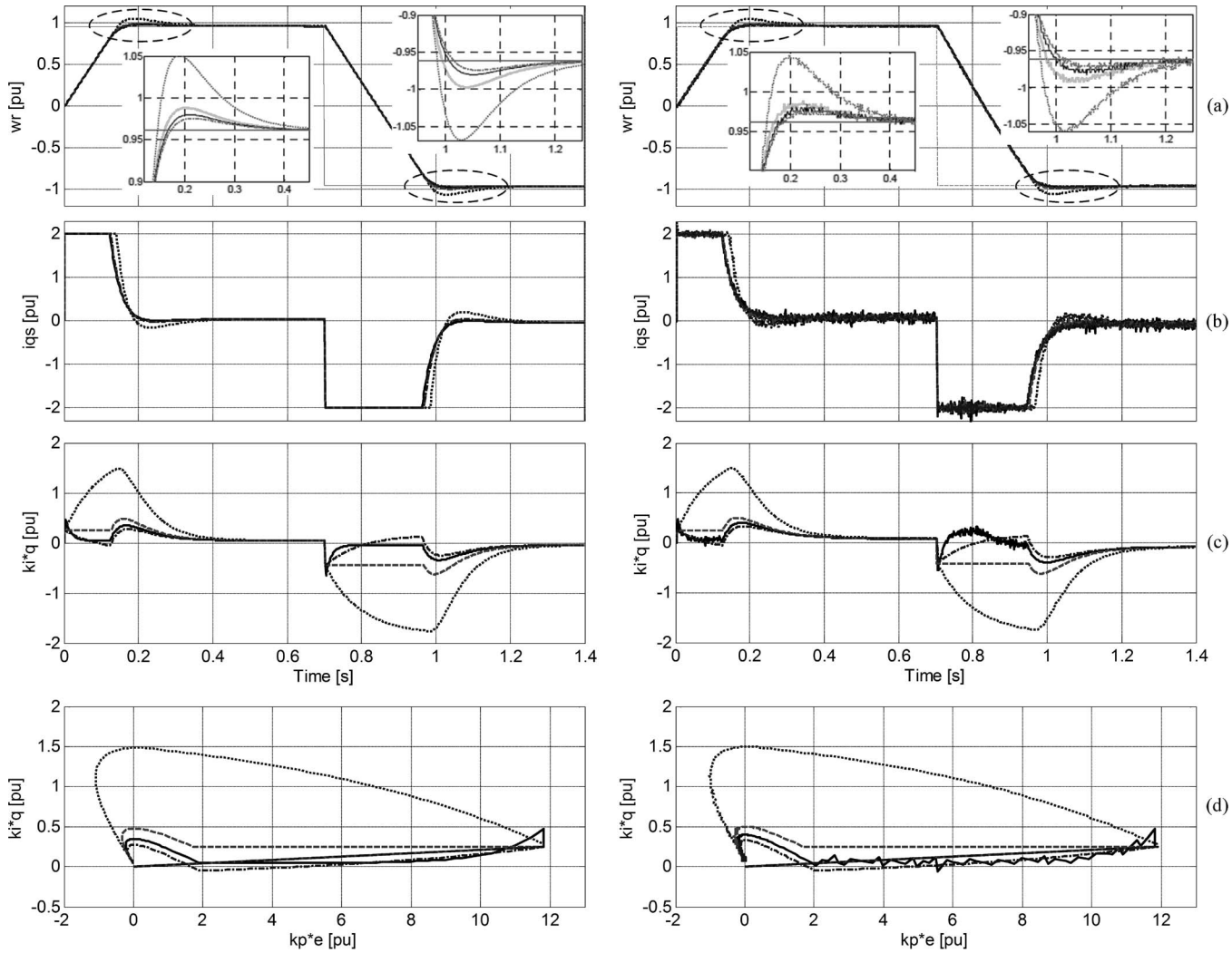

Fig. 7. Simulated (left) and experimental (right) comparison of anti-windup PID schemes under no load (dotted: tracking back calculation, dashed: conditional integration, dash-dotted: combined scheme, solid: proposed scheme). (a) Speed. (b) Current. (c) Integral control. (d) Error trajectory on PI plane.

Matlab/Simulink and the same parameter values in Table I. The experimental waveforms are almost the same as the simulated ones. Because the steady-state value of the integral state is near the initial value of zero at no load, the integral state traces of each scheme (except the tracking back calculation) are almost the same as shown in Fig. 7(c) and (d), and the speed responses, too, perform similarly as shown in Fig. 7(a). For the tracking back calculation method, the integral state increases during the saturation range and its value is larger than the steady-state value when the PID control enters in the linear range. Hence, larger overshoot occurs in the speed response.

Fig. 8 shows simulated and experimental results under full load. The experimental waveforms are similar to the simulated ones. At full load, the steady-state value of the integral state is larger than the initial value as shown in Fig. 8(c) and (d). Since the integral states of the conditional integration and combined schemes, at the beginning of the linear range, are smaller than the steady-state values, the overdamped speed responses are obtained as shown in Fig. 8(a). For the tracking back calculation method, the integral state value is larger than the steady-state value when the controller begins to operate in the linear range. Compared to the no-load case, the difference between the integral state values is less and overshoot becomes smaller in the speed response at full load. With the proposed method, the steady-state value of the integral state is properly predicted and is utilized as an initial value when the PID control enters the linear range. Hence, speed responses are almost identical in the linear range without respect to load conditions or step reference change.

IV. Conclusion

The integral windup has been analyzed on the PI plane, and the anti-windup PID control scheme for variable-speed motor drives has been proposed to overcome the windup phenomenon. The proposed anti-windup scheme has been compared with conventional methods through simulation and experimental results of the speed control of a vector-controlled induction motor driven by a PWM-VSI. The rise time is mainly determined by controller output limitations during the saturation range, while the overshoot and steady-state error performance depends only on PID gain during the linear range. Hence, speed response can be designed by choosing the PID gain and the designed

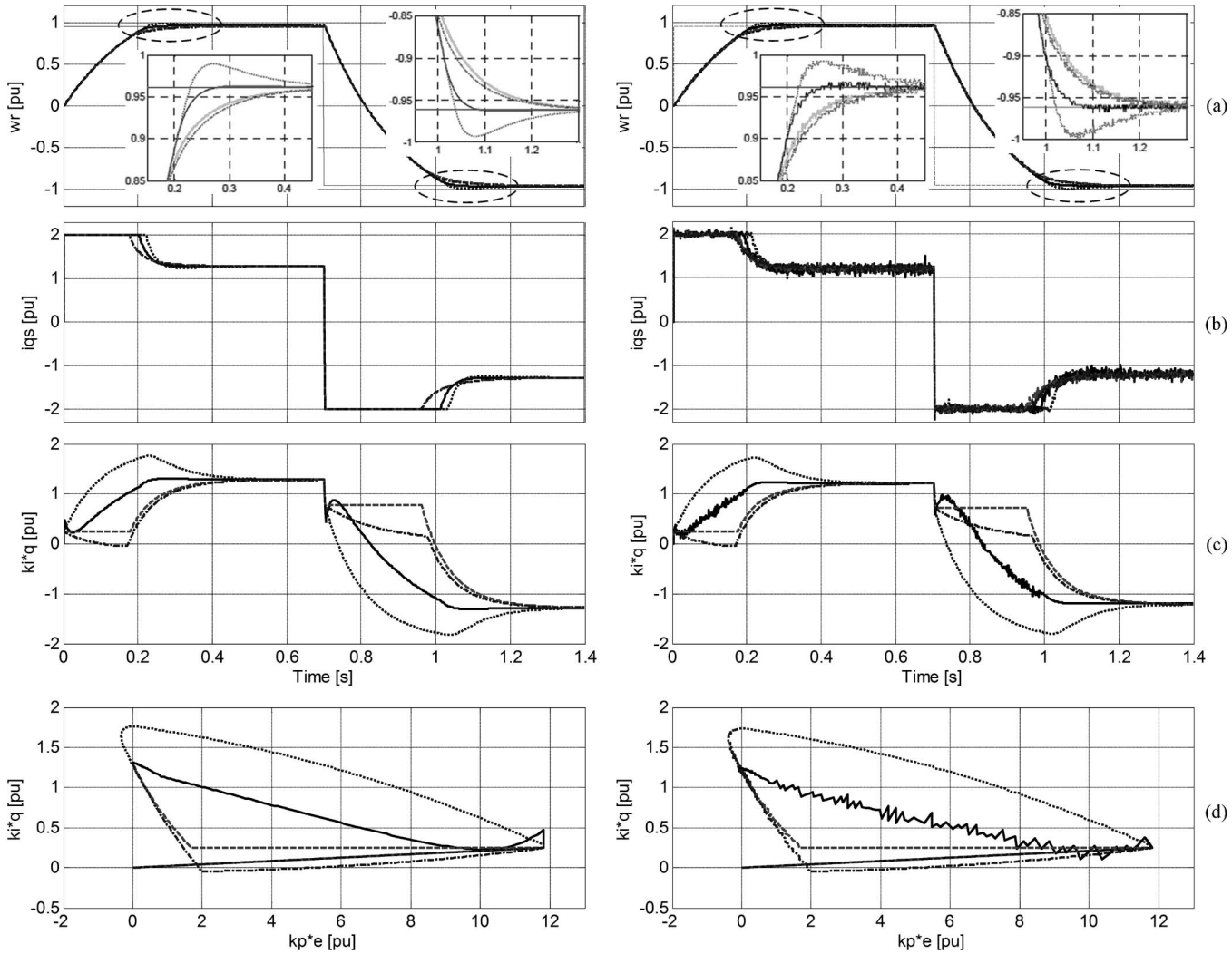

Fig. 8. Simulated (left) and experimental (right) comparison of anti-windup PID schemes under full load (dotted: tracking back calculation, dashed: conditional integration, dash-dotted: combined scheme, solid: proposed scheme). (a) Speed. (b) Current. (c) Integral control action. (d) Error trajectory on PI plane.

response can be obtained without respect to load conditions. With the proposed anti-windup scheme, more similar control performance such as overshoot and settling time determined by PID gain, can be obtained over conventional anti-windup techniques.

REFERENCES

[1] K. Astrom and T. Hagglund, *PID Controllers: Theory, Design, and Tuning*. Research Triangle Park, NC: ISA, 1995, pp. 59–92.

[2] S. Tarbouriech and M. Turner, "Anti-windup design: An overview of some recent advances and open problems," *IET Control Theory Appl.*, vol. 3, no. 1, pp. 1–19, Mar. 2009.

[3] B. Bahrani, S. Kenzelmann, and A. Rufer, "Multivariable-PI-based dq current control of voltage source converters with superior axes decoupling capability," *IEEE Trans. Ind. Electron.*, vol. 58, no. 7, pp. 3016–3026, Jul. 2011.

[4] R. J. Wai, J. D. Lee, and K. L. Chuang, "Real-time PID control strategy for Maglev transportation system via particle Swarm optimization," *IEEE Trans. Ind. Electron.*, vol. 58, no. 2, pp. 629–646, Feb. 2011.

[5] J. W. Choi and S. C. Lee, "Antiwindup strategy for PI-type speed controller," *IEEE Trans. Ind. Electron.*, vol. 56, no. 6, pp. 2039–2046, Jun. 2009.

[6] J. K. Seok, K. T. Kim, and D. C. Lee, "Automatic mode switching of P/PI speed control for industry servo drives using online spectrum analysis of torque command," *IEEE Trans. Ind. Electron.*, vol. 54, no. 5, pp. 2642–2647, Oct. 2007.

[7] J. K. Seok, "Frequency-spectrum-based antiwindup compensator for PI controlled systems," *IEEE Trans. Ind. Electron.*, vol. 53, no. 6, pp. 1781–1790, Dec. 2006.

[8] K. Ohishi, E. Hayasaka, T. Nagano, M. Harakawa, and T. Kanmachi, "High-performance speed servo system considering voltage saturation of a vector-controlled induction motor," *IEEE Trans. Ind. Electron.*, vol. 53, no. 3, pp. 795–802, Jun. 2006.

[9] R. Hanus, M. Kinnaert, and J. L. Henrotte, "Conditioning technique, a general anti-windup and bumpless transfer method," *Automatica*, vol. 23, no. 6, pp. 729–739, Nov. 1987.

[10] Y. Peng, D. Vrancic, and R. Hanus, "Anti-windup, bumpless, and conditioned transfer techniques for PID controllers," *IEEE Control Syst.*, vol. 16, no. 4, pp. 48–57, Aug. 1996.

[11] K. S. Walgama, S. Ronnback, and J. Sternby, "Generalization of conditioning technique for anti-windup compensators," *Proc. Inst. Elect. Eng.*, vol. 139, pt. D, no. 2, pp. 109–118, Mar. 1992.

[12] A. S. Hodel and C. E. Hall, "Variable-structure PID control to prevent integrator windup," *IEEE Trans. Ind. Electron.*, vol. 48, no. 2, pp. 442–451, Apr. 2001.

[13] H. B. Shin, "New antiwindup PI controller for variable-speed motor drives," *IEEE Trans. Ind. Electron.*, vol. 45, no. 3, pp. 445–450, Jun. 1998.

[14] J. G. Park, J. H. Chung, and H. B. Shin, "Anti-windup integral-proportional controller for variable-speed motor drives," *J. Power Electron.*, vol. 2, no. 2, pp. 130–138, Apr. 2002.

[15] N. J. Krikelis, "State feedback integral control with intelligent integrator," *Int. J. Control*, vol. 32, no. 3, pp. 465–473, 1980.

[16] D. W. Novotny and R. D. Lorenz, *Introduction to Field Orientation and High Performance AC Drives*. New York: IEEE Press, 1986.

Hwi-Beom Shin (SM'86–M'95) was born in Seoul, Korea, in 1958. He received the B.S. degree in electrical engineering from Seoul National University, Seoul, Korea, in 1982, and the M.S. and Ph.D. degrees in electrical engineering from Korea Advanced Institute of Science and Technology, Seoul, Korea, in 1985 and 1992, respectively.

He was with Hyundai Electronics Industries Co. Ltd. as a Chief Engineer, from 1990 to 1992. Since 1993, he has been with the Department of Electrical Engineering, Gyeongsang National University, Jinju, Korea, where he is a Professor and a Researcher of Engineering Research Institute. His research interests are in the areas of power electronics and control, electric vehicle, and industrial drives.

Dr. Shin is a member of the IEEE Power Electronics and Industrial Electronics Societies.

Jong-Gyu Park received the B.S., M.S., and Ph.D. degrees in electrical engineering from Gyeongsang National University, Jinju, Korea, in 1995, 1997, and 2004, respectively.

He is currently a full-time Lecturer in the Department of Electricity, Gyeongnam Provincial Namhae College, Gyeongnam, Korea. His research interests are in the areas of power electronics, ac machine drives, and microcontroller-based control applications.